

RESEARCH ARTICLE

10.1002/2015WR016936

Special Section:

The 50th Anniversary of Water Resources Research

Key Points:

- Method to predict hydraulic behavior in estuaries
- Method to predict salt intrusion in estuaries

Correspondence to:

H. H. G. Savenije,
h.h.g.savenije@tudelft.nl

Citation:

Savenije, H. H. G. (2015), Prediction in ungauged estuaries: An integrated theory, *Water Resour. Res.*, 51, doi:10.1002/2015WR016936.

Received 21 JAN 2015

Accepted 17 MAR 2015

Accepted article online 24 MAR 2015

Prediction in ungauged estuaries: An integrated theory

Hubert H. G. Savenije¹¹Water Resources Section, TU-Delft, Delft, Netherlands

Abstract Many estuaries in the world are ungauged. The International Association of Hydrological Sciences completed its science decade on Prediction in Ungauged Basins (PUB) in 2012 (Hrachowitz *et al.*, 2013). Prediction on the basis of limited data is a challenge in hydrology, but not less so in estuaries, where data on fundamental processes are often lacking. In this paper, relatively simple, but science-based, methods are presented that allow researchers, engineers, and water managers to obtain first-order estimates of essential process parameters in estuaries, such as the estuary depth, the tidal amplitude, the tidal excursion, the phase lag, and the salt water intrusion, on the basis of readily obtainable information, such as topographical maps and tidal tables. These apparently simple relationships are assumed to result from the capacity of freely erodible water bodies to adjust themselves to external drivers and to dissipate the free energy from these drivers as efficiently as possible. Thus, it is assumed that these systems operate close to their thermodynamic limit, resulting in predictable patterns that can be described by relatively simple equations. Although still much has to be done to develop an overall physics-based theory, this does not prevent us from making use of the empirical “laws” that we observe in alluvial estuaries.

1. Introduction

1.1. Estuaries as Essential Life Support Systems

Estuaries form essential parts of the human–earth system. They are intensively used to sustain a wide range of economic activities. In rapidly urbanizing coastal areas, estuaries are both a crucial resource and a support system for human settlements, agriculture, transport, and ecosystem services. As the connecting element between ocean and river, estuaries have properties of both: they contain both fresh and saline water; they experience tides, but also river floods; and they host both saline and fresh ecosystems. But more importantly, they have unique properties of their own: a unique brackish aquatic environment and hydrodynamic behavior different from all other water bodies.

Being such a crucial element of the terrestrial system, one would expect that estuaries are intensively gauged worldwide, but this is rarely the case. Only the most intensively used estuaries are closely monitored, particularly if they form part of a busy navigation network. But most estuaries in the world are poorly gauged, in the sense that we hardly know their geometry (depth, slope, and cross-sectional properties) or the amounts of freshwater and sediments that they receive. If there is information on tidal water levels, then this is seldom measured continuously or at more points along the estuary. Consistent information on salinity, water quality, ecology, and morphology is generally lacking, even in the more intensively inhabited estuaries and deltas. This is not so strange because the intensive, consistent, and permanent monitoring of estuaries is both costly and difficult. So, if science can help to estimate essential physical properties of estuaries with readily available or easily obtainable information then this would be an important contribution to society.

1.2. The Paradox of Simplicity

Because estuaries are such complex systems, where so many different physical and biological processes interact, one would expect that only the most complex models would be able to describe estuary behavior, but here we see a remarkable paradox. Estuaries manifest surprisingly simple behavior, particularly alluvial estuaries, where the water body has been able to modify its shape in a way that it can efficiently absorb and evacuate flood waters and sediments from the terrestrial system, as well as the energy fluxes generated by the oceans in the form of tides, waves, and storm surges.

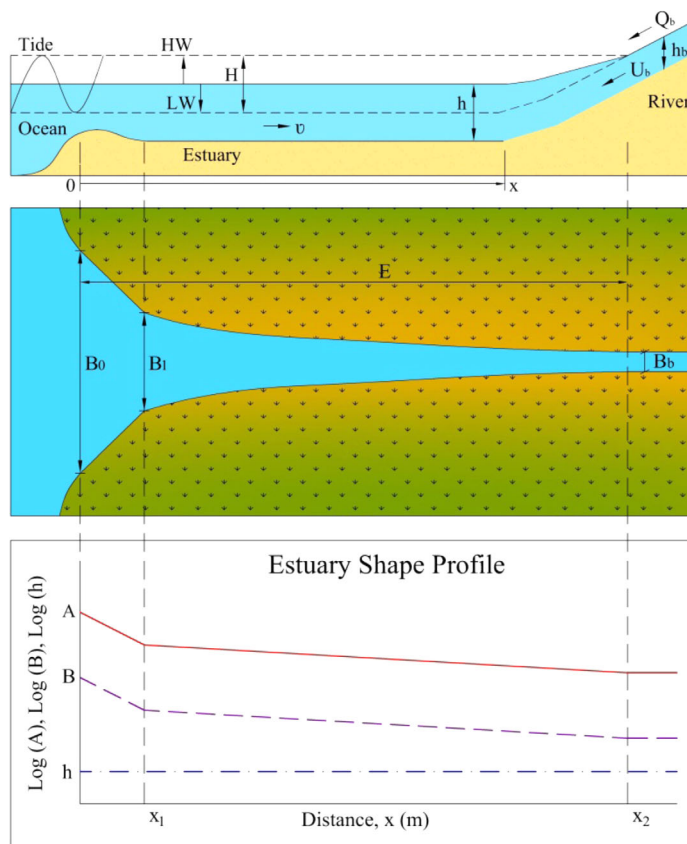


Figure 1. Definition sketch showing the exponentially varying width and cross-sectional area and the inflection point at x_1 . A is the cross-sectional area, B is the width, and h is the depth. H is the tidal range, the vertical distance between high water (HW) and low water (LW). v is the tidal velocity amplitude. U_b , h_b , B_b , and Q_b are the bankfull velocity, depth, width, and discharge at the transition point of estuary to river.

The most evident manifestation of this simplicity is the shape of alluvial estuaries. The cross-sectional areas of alluvial estuaries, when plotted against the longitudinal axis, follow an exponential function, and so does the surface width. Moreover, in long alluvial estuaries (with a length longer than about half a wave length), there appears to be almost no bottom slope and the amplitude of the tidal velocity is almost constant along the estuary axis. This surprisingly simple behavior only occurs if the system is able to adjust its shape to external drivers (i.e., in alluvial estuaries) and not in estuaries with fixed boundaries, such as fjords and sounds. Figure 1 is a schematic representation of an alluvial estuary, but Figure 2 presents a selection of real estuaries, where the geometry is plotted on semilogarithmic paper, demonstrating straight lines. A larger selection of estuaries and more detailed information can be found on the web site www.salinityandtides.com.

The physical explanation for this apparent behavior is not trivial, but is probably related to the most efficient way in which alluvial systems organize their energy dissipation. This hints toward optimality associated with maximum entropy production [e.g., Kleidon *et al.*, 2013]. When a system operates close to its thermodynamic limit of maximum power [Kleidon and Renner, 2013; Kleidon *et al.*, 2014], a complex physical system may demonstrate predictable and simple behavior. Although, as yet, there is no consistent theory to derive this “optimal shape” from basic physical principles, it does not prevent us from using the patterns we observe empirically. Moreover, the exponential function is a very attractive equation to be used in the solution of differential equations, and as such, nature has done us a great favor.

In the book “Salinity and Tides in Alluvial Estuaries,” Savenije [2005, 2012] presented a range of analytical solutions of the fundamental equations for hydraulics, tidal mixing, and salt intrusion that have practical applicability in alluvial estuaries and that can be used if only limited information is available. The book

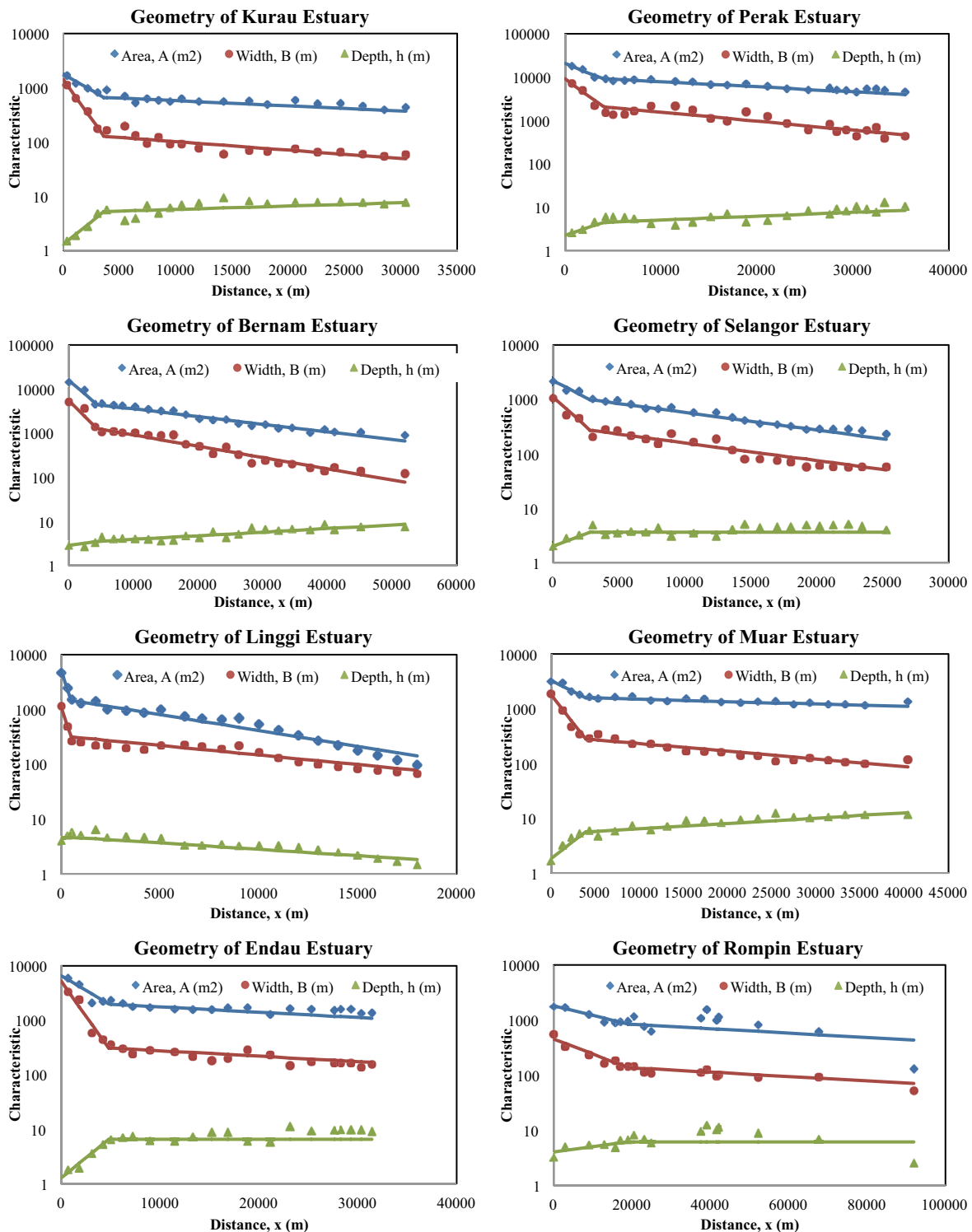


Figure 2. Variation of the cross-sectional area (A), width (B), and cross-sectional average depth (h) of 28 estuaries, plotted on semilogarithmic paper.

makes ample use of the literature and is based on many field investigations carried out in estuaries in different parts of the world (downloadable from www.salinityandtides.com). In this overview article, we do not present and discuss the underlying material in detail, but rather focus on how this theory can be applied in situations where limited information is available.

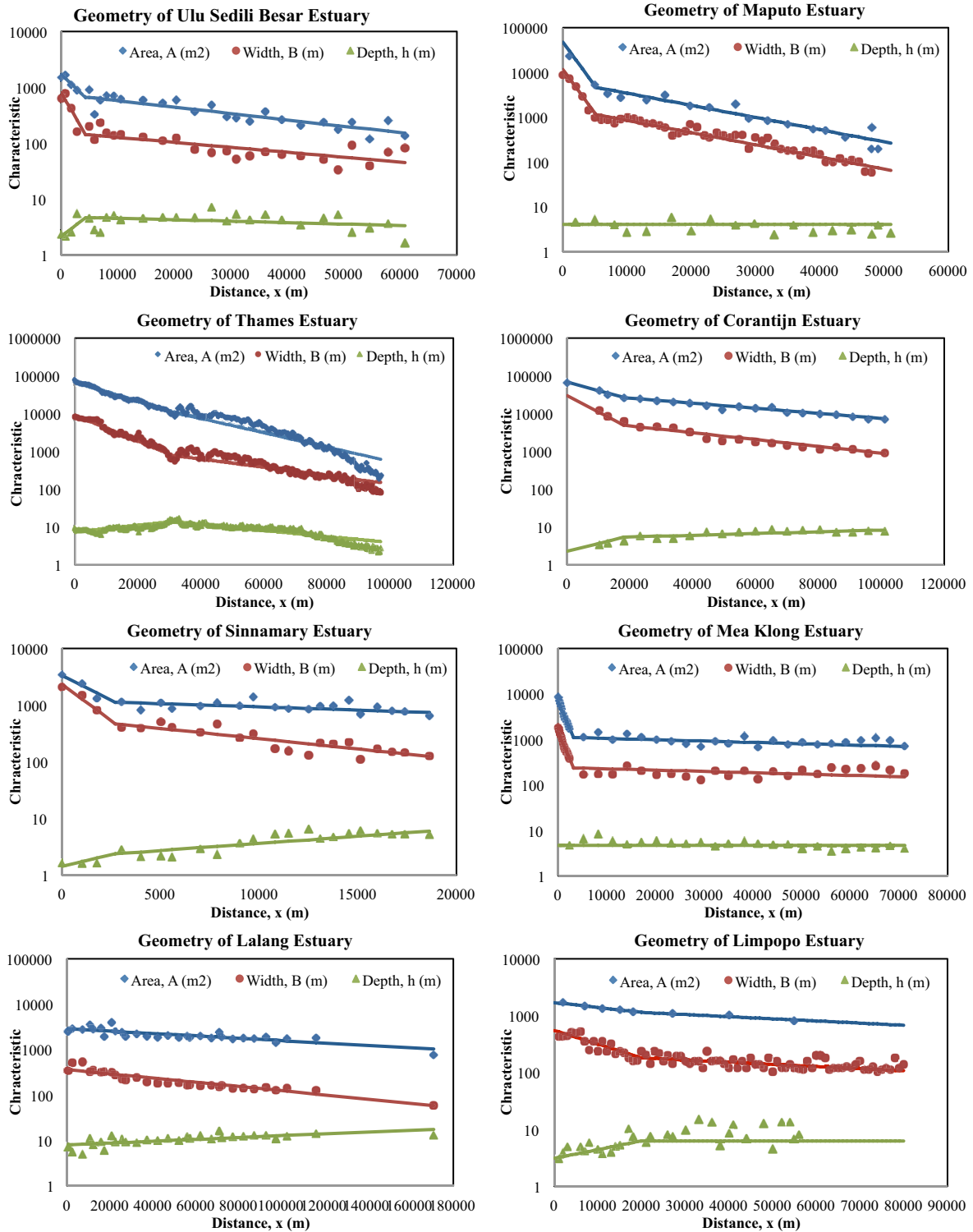


Figure 2. (Continued)

1.3. The Predictability of Estuarine Behavior

Not only is the behavior of alluvial estuaries surprisingly simple, it also appears to be predictable. One important property of alluvial estuaries is that the amplitude of the tidal velocity at spring tide (cross-sectional average) is approximately 1 m/s, throughout the estuary. This is a remarkable property that Bruun

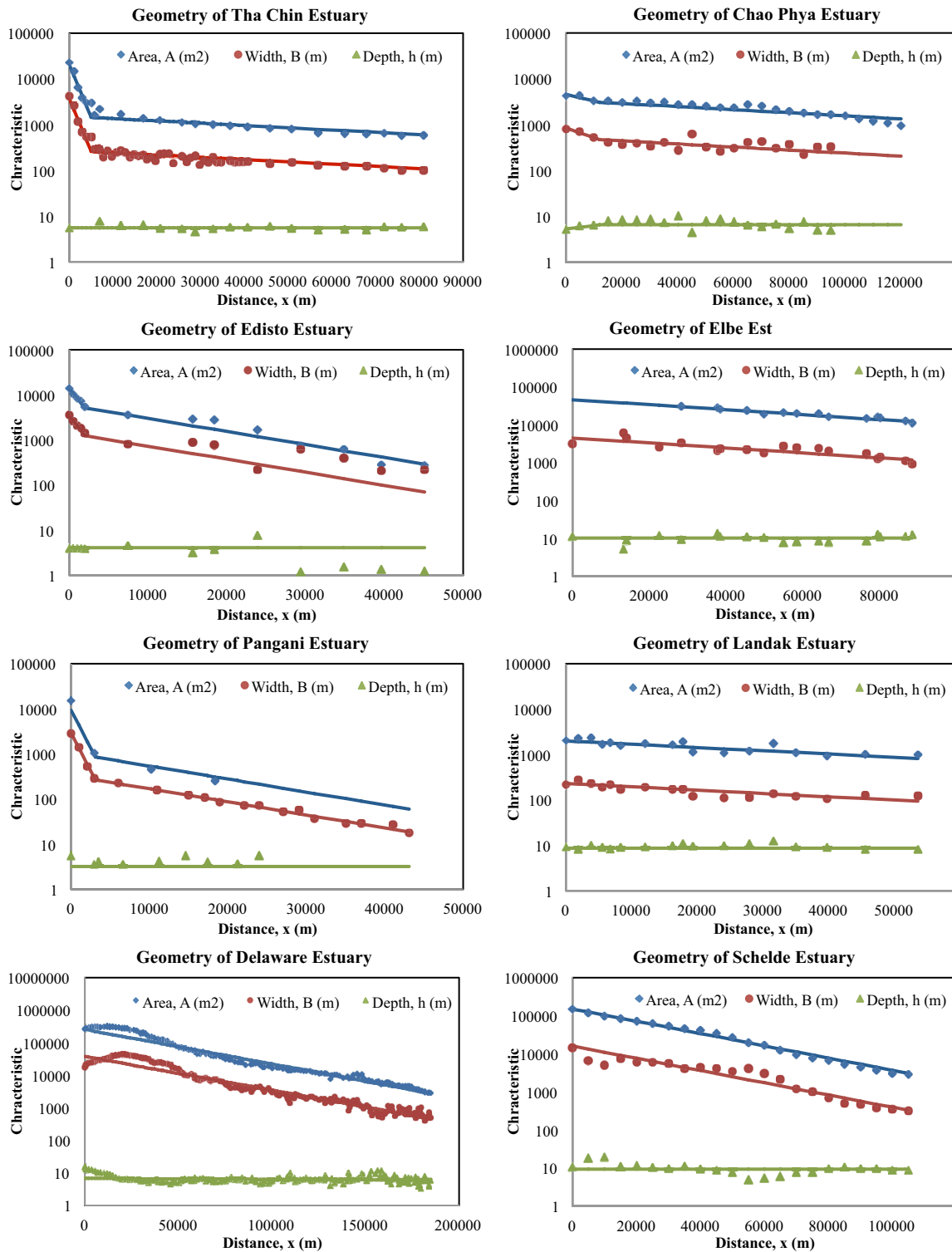


Figure 2. (Continued)

and Gerritsen [1960] showed to be valid for tidal inlets, but which also appears to apply to the entire tidal region of alluvial estuaries. Cai and Savenije [2013] showed that the tidal amplitude and associated velocity amplitude in estuaries have asymptotic values toward which they converge at some distance from the estuary mouth. This asymptotic situation corresponds to an “ideal estuary,” where there is no tidal damping and

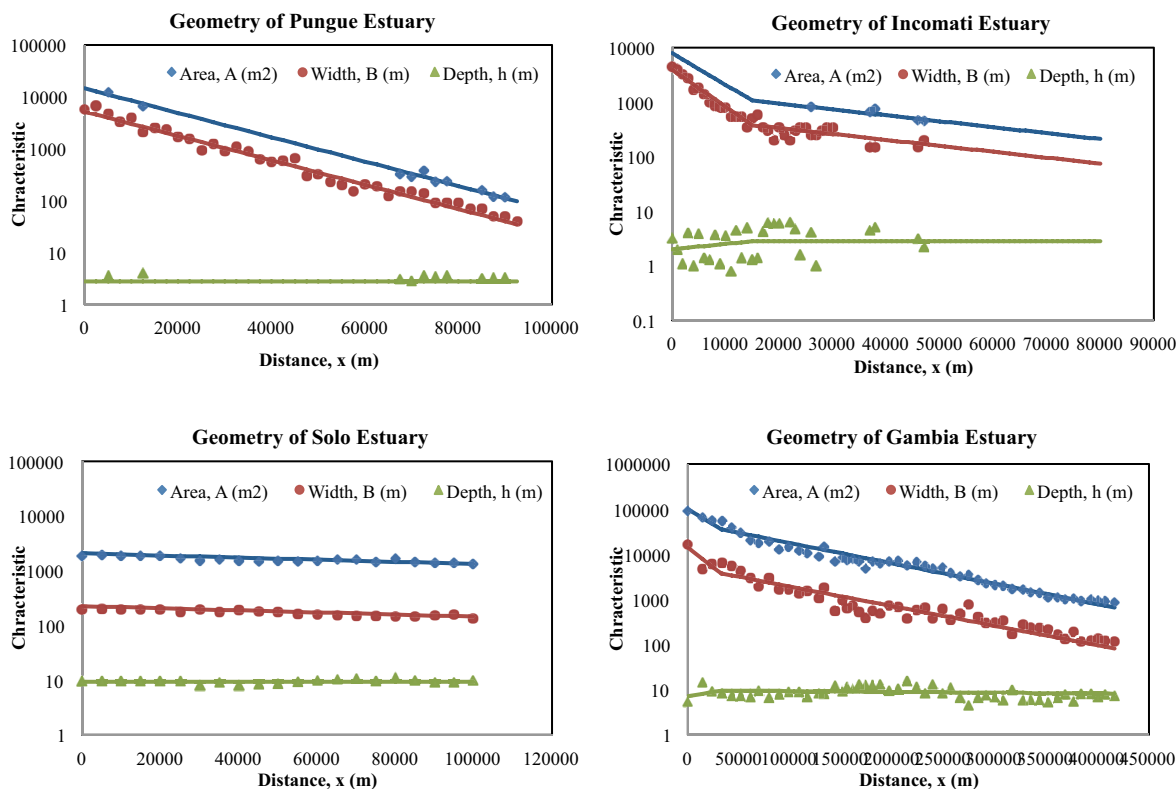


Figure 2. (Continued).

where the celerity of the tidal wave is the same as in a frictionless channel with constant cross section (equal to $c_0 = \sqrt{gh}$). This is the more remarkable, because natural estuaries are neither prismatic (they have an exponentially varying cross section) nor frictionless. *Savenije and Veling* [2005] showed that estuaries that are dredged, and hence are deeper than under natural circumstances, have amplified tidal waves that progress faster than c_0 , as is the case in, for instance, the Scheldt, the Elbe, and other dredged estuaries. But in ungauged estuaries, where the economic use is—not by chance—less intensive, the morphology is generally more natural and the ideal estuary condition may be assumed to apply, at least in the part of the estuary that is not significantly affected by the river discharge (where the tidal velocity amplitude is an order of magnitude larger than the freshwater velocity).

This offers opportunities for prediction in poorly gauged estuaries. If the hydraulic behavior and the geometry are predictable, then also the salinity intrusion can be modeled with limited uncertainty. For the modeling and prediction of salt intrusion, however, predictive equations are needed that provide estimates of essential parameters that describe tidal mixing. But fortunately also these can be found in alluvial estuaries [*Savenije*, 1993], probably as a result of the same energetic optimum that is responsible for the exponential shape of estuaries, but this is still speculation.

1.4. The Need for an Integrated Theory and the Giant's Perspective

Although there is still fundamental research required to answer the question why alluvial estuaries demonstrate such predictable behavior, there is already practical use that we can make of the “laws” and patterns that we observe empirically. Condition is that we consider an estuary as an integrated system, whereby its shape, tidal hydraulics, and salt intrusion are intertwined and cannot be considered in isolation. For these “laws” to apply, we have to consider the system as a whole and not to consider the processes in too much detail. We have to zoom out to the macroscale where the processes have had the opportunity to cancel out local-scale variability. Simplicity and predictability only manifest themselves at the system scale while locally there may be (temporary) deviations from the expected values.

The shape being the crucial boundary condition for hydraulics and salt intrusion, the next section is dedicated to estuary shape. Because the paper aims at providing estimates for ungauged estuaries, we assume

the ideal estuary condition to apply. The subsequent two sections present the tidal hydraulics and the salt intrusion, while the final section presents a summary and a discussion.

2. Estuary Shape and What We Can Read From it

Over time, alluvial estuaries develop their geometry in a state of (intermediate) dynamic equilibrium that allows terrestrial and oceanic free energy to dissipate efficiently. *Kleidon et al.* [2013] demonstrated that the terrestrial morphology can be explained by thermodynamic principles and gave a plausible explanation for patterns that appear in freely erodible systems. They indicated that the (self)-organization of structures in the terrestrial system could be explained by maximum entropy production and optimality of energy expenditure, close to the thermodynamic limit. Something similar is happening in alluvial estuaries, although the precise formulation in thermodynamic terms still needs to be done. What we know empirically is that alluvial estuaries tend toward an exponentially varying cross section and width, and, if the estuary is long enough, a constant tidal average depth. This exponential shape causes the tidal velocity amplitude to be virtually constant along the estuary axis, and allows the development of an asymptotic situation of constant tidal amplitude, which corresponds to an ideal estuary [*Cai and Savenije*, 2013]. As a result, the amount of free kinetic and potential energy per unit volume of estuary water is constant along the estuary axis, which corresponds to the “most likely state” of a system in dynamic equilibrium.

Generally, estuaries can be schematized in one or two segments each with a different convergence length (see Figure 1). As a result, the following equations apply:

$$A = A_i \exp\left(-\frac{(x-x_i)}{a_i}\right) \quad (1)$$

$$B = B_i \exp\left(-\frac{(x-x_i)}{b_i}\right) \quad (2)$$

where the subscript i indicates properties of the different segments, A and B are the cross-sectional area and width, and a_i and b_i are the convergence length of the cross-sectional area and width, respectively. The point x_i is the position of the (internal) boundary and A_i and B_i are the values at the (internal) boundary. If the convergence lengths of A and B are the same, then there is no bottom slope. If they are different, then there is an exponential variation of the depth with a convergence length equal to $ab/(a-b)$. Often we see that the exponential shape has two segments, a short part of less than 10 km close to the ocean with a short convergence length, and then, after a well-defined inflection point (at $x = x_1$), the second reach with a longer convergence length. The second reach tends exponentially to the river width B_b . Formally, this would imply an adjustment of equations (1) and (2) subtracting the river cross section and width from the parameters A and B , but in the part of the estuary where salt intrusion occurs, this adjustment has a minor influence. Figure 2 presents an illustration of this geometry for a selection of real estuaries [from *Gisen*, 2015]. In Table 1, the geometric data of a large collection of estuaries is presented, where the subscript 0 refers to the estuary mouth or the first reach. The subscript 1 refers to the inflection point or to the second estuary reach.

2.1. What Determines the Shape?

The estuary shape is obviously the result of the interaction between the river discharge and the tide. But what are the characteristic values of river discharge and tide that determine it, and which of the shape parameters do each of them determine? The regime theory of alluvial rivers offers an opening. *Gisen et al.* [2015] showed that the upstream geometry of the estuary (essentially the depth and the width) is determined by the bankfull discharge, in agreement with the regime theory of *Lacey* [1930] and *Simons and Albertson* [1960].

Regime theory links the width to the bankfull discharge through the famous formula of Lacey:

$$B_b = k_s Q_b^{0.5} \quad (3)$$

where Q_b is the bankfull discharge and the factor k_s depends on the sediment composition. *Gisen et al.* [2015] used data from 23 estuaries to test these relationships and found:

Table 1. Characteristics of a Selection of Estuaries^a

No	Estuary	A_1 (10^3 m ²)	a_1 (km)	B_1 (m)	B_f (m)	b_1 (km)	h_1 (m)	x_1 (km)	H_0 (m)	T (h)
1	Kurau	0.7	46	130	20	28	6.2	3.6	2.3	12.4
2	Perak	9.2	37	2,070	130	21	6.3	4	2.8	12.4
3	Bernam	4.5	25	1,270	45	17	5.3	4.3	2.9	12.4
4	Selangor	1	13	270	35	13	3.7	2.8	4.0	12.4
5	Linggi	1.5	8	320	25	13	3.2	0.5	2.0	12.4
6	Muar	1.6	100	280	55	31	8.2	3.9	2.0	12.4
7	Endau	2	44	310	72	44	6.5	4.8	1.9	12.4
8	Rompin	0.8	110	140	50	110	6.1	19	2.5	12.4
9	Ulu Sedili Besar	0.7	38	140	35	49	4.1	4.3	2.5	12.4
10	Maputo	4.7	16	1,150	100	16	4.1	5.1	3.3	12.4
11	Thames	10.9	23	780	50	40	8.2	31	5.3	12.4
12	Corantijn	26.8	64	5,000	400	48	6.7	18	3.1	12.4
13	Sinnamary	1.1	39	470	95	12	3.9	2.7	3.3	12.4
14	MaeKlong	1.1	150	240	150	150	4.6	3.2	3.6	12.4
15	Lalang	2.9	167	360	130	94	10.3	0	2.6	24
16	Limpopo	1.1	115	180	90	115	6.3	20	1.9	12.4
17	Tha Chin	1.4	87	260	45	87	5.6	5.0	2.6	12.4
18	ChaoPhya	3.1	130	470	200	130	6.5	12	3.4	24
19	Edisto	5.2	15	1,250	60	15	4.1	2.0	3.2	12.4
20	Elbe	43	66	2,880	350	50	11.7	0	4.6	12.4
21	Pangani	0.9	15	270	35	15	3.2	3.1	4.2	12.4
22	Landak	2	60	230	100	60	8.7	0	1.6	24
23	Delaware	255	41	37,655	120	42	6.4	0	1.8	12.4
24	Schelde	150	27	16,000	50	27	9.4	0	4.0	12.4
25	Pungue	14.5	19	5,200	50	19	2.8	0	6.7	12.4
26	Incomati	1.1	40	380	22	40	2.8	15	3.3	12.4
27	Solo	2.1	226	225	95	226	9.2	0	1.8	24
28	Gambia	35.7	96	3,700	110	100	8.8	33	1.83	12.4

^aFor location and more data, see www.salinityandtides.com. Note: H_0 is the tidal range (twice the tidal amplitude) at the estuary mouth, during spring tide.

$$B_b = 3.74Q_b^{0.467} \tag{4}$$

with a correlation $R^2 = 66\%$. For the regime discharge, *Gisen et al.* [2015] used the annual maximum discharge with a return period of 1.5 years. Given the uncertainty in the determination of the bankfull discharge, this is a good correlation and well in agreement with Lacey’s equation.

2.2. Depth

In addition, they derived an expression for the depth, assuming the ideal estuary conditions to apply, with a correlation of 62%:

$$h_1 = 0.69Q_b^{0.31} \tag{5}$$

Using (4), this implies that:

$$h_1 = 0.28B_b^{0.67} \tag{6}$$

where the exponent 0.67 corresponds with the one found in regime theory [e.g., *Cao and Knight*, 1996].

Knowing the depth at the upstream end appears to be the key to knowing the depth of the entire estuary segment. *Gisen et al.* [2015] showed that the depth at the upstream boundary determines the depth of the estuary in the upstream reach, the slope in the tidal region being minor. This is an important finding for ungauged estuaries, because it allows us to estimate the estuary depth from a map, using equation (6), simply by measuring the stream width at the limit of the tidal influence.

2.3. Convergence

But what determines the convergence? Intuitively we feel that the convergence results from the balance between the strength of the river discharge and the tide. If an estuary is riverine (determined by large river discharge and limited tidal influence), we expect the estuary to be more prismatic (to have a long convergence length), such as we see in the branches of delta systems. If however the tidal influence is much stronger than the river discharge, we expect a pronounced funnel shape. The proportion of the amount of

freshwater entering the estuary during a tidal period to the tidal prism P (the volume of saline water entering the estuary during a tidal period) is the Canter-Cremers number. For bankfull discharge, this amount equals $Q_b T$. The tidal prism at the inflection point can be approximated by $B_1 h_1 v_1 T / \pi$ [see Savenije, 2012]. Moreover, Q_b is proportional to B_b ($Q_b = U_b h_b B_b$), Hence, the Canter-Cremers number for bankfull flow at the inflection point can be written as:

$$\frac{Q_b T}{P} = \frac{Q_b T}{B_1 v_1 h_1 T} \pi = \frac{B_b U_b h_b T}{B_1 v_1 h_1 T} \pi = k_b \pi \left(\frac{B_b}{B_1} \right) \quad (7)$$

where k_b is a proportionality factor, defined by:

$$k_b = \frac{U_b h_b}{v_1 h_1} \quad (8)$$

which under regime condition is expected to be constant, the regime condition being a bankfull flood at the upstream boundary and an extreme spring tide with a velocity amplitude of 1 m/s at the inflection point. A constant value of k_b indeed appears to apply, and Gisen *et al.* [2015] found that with $k_b = 1.44$, a high correlation was found of $R^2 = 80\%$ for the ideal estuary assumption. This factor implies that under bankfull conditions, the river velocity would be about 1.4 m/s (since h_b and h_1 are expected to be equal).

Hence, we can conclude that the bankfull discharge determines the depth of the estuary and that the proportion between freshwater and saline water, under regime conditions, determines the width ratio and hence the convergence (note: the convergence length b is the ratio of the estuary length to the natural logarithm of the width ratio).

2.4. Bottom Slope

In long open-ended estuaries, there is not expected to be a bottom slope, at least not in an equilibrium situation. An estuary which is shorter than a quarter of the wave length generally has a significant bottom slope (a significant depth convergence length whereby $b > a$), even though the cross-sectional area still obeys an exponential function. In these estuaries, we cannot read the depth from the regime width. But in long (not dredged) alluvial estuaries, we can. If there is a slope, as can be seen in several estuaries in Figure 2, then this slope is generally modest and probably reflects an intermediate situation, where the estuary is restoring the balance between tide and river-dominated regime. Apparently, a tide-dominated regime is likely to cause landward shallowing (e.g., Linggi), while a river-dominated regime may cause an inverse slope (e.g., Muar, Lalang, and Sinnamary). The inverse slope is likely the result of a recent flood, where the high sediment carrying capacity in the upstream narrow part of the estuary causes bottom erosion, while sediments deposit further down as the estuary becomes wider. If there is a long enough period without floods, then this inverse slope may be expected to gradually level out. Similarly, landward shallowing may be the result of gravitational circulation, carrying marine sediments inland, with insufficient floods to flush it back out. Whether these slopes have a more permanent or temporal character depends on the time scales of these processes.

In closed estuaries, a bottom slope may occur near the natural limit or a closure structure. At an obstruction, a standing wave occurs, where the tidal velocity is zero. As a result, we observe shallowing at the foot of a closure structure (e.g., in the Thames and the Scheldt estuary). But even if there is an obstruction in a convergent estuary, the fact that the reflected wave loses its energy quickly, due to divergence, causes the area of influence of the obstruction to be relatively small (10–20 km depending on the convergence).

3. Predicting the Tidal Hydraulics on the Basis of Estuary Shape

In predicting tidal hydraulics, we make use of the analytical solutions of the St. Venant equations, as provided by Savenije *et al.* [2008]. These equations are only applicable in open-ended estuaries where there is no reflected wave, or in estuaries where the tidal barrier is sufficiently far removed from the area of interest (see H. Cai *et al.*, An analytical approach to determining resonance in semi-closed convergent estuaries, submitted to *Journal of Geophysical Research: Oceans*, 2015). The four equations are summarized in dimensionless form in Appendix A, presenting the governing equations and the definitions of the

dimensionless variables in equations (A1)–(A2). Also the dimensional variables are explained in Appendix A.

If observations of tidal water levels are available at a number of locations, then the tidal damping and the tidal amplitude can be determined at different places, which allows solution of these equations, given that the geometry is known.

In an ungauged estuary, the cross-sectional convergence is not known, and one has to assume that the cross-sectional convergence length a equals the width convergence length b , which in fact is the assumption of no bottom slope. Since in an ungauged estuary, there is, by definition, no observation of the tidal damping, we assume the condition of an ideal estuary, where there is no damping and the tidal wave propagates with the classical wave celerity c_0 ($\delta = 0$ and $\lambda = 1$). In long alluvial estuaries, this is an acceptable premise, particularly for the second segment. This leads to the following rather simple hydraulic equations (the parameters are explained in Appendix A):

$$\mu^2 = \frac{1}{\gamma^2 + 1} \quad (9)$$

$$\tan \varepsilon = \gamma^{-1} \quad (10)$$

In addition, the condition of zero damping ($\delta = 0$, $\lambda = 0$) leads to $\gamma = \chi\mu^2$, which translates into:

$$C^2 = \frac{v^2 b_1}{\eta h_1} \quad (11)$$

In dimensional form, equation (9) can be written as:

$$\frac{v}{\eta} = r_s \frac{\omega b_1}{h_1} \sqrt{\frac{c_0^2}{c_0^2 + \omega^2 b_1^2}} \quad (12)$$

For given width convergence and tidal period, an estimated storage width ratio (a good guess is $r_s \approx 1.1$), and a depth estimate by equation (6), equation (12) provides a relation between the amplitudes of the tidal water level and tidal velocity. This equation can be used for different purposes, for instance, to compute the tidal excursion ($E = vT/\pi$) for a given certain value of η , required for the salt intrusion calculation. Another application would be to check the depth estimate made by equation (6). If we assume that during spring tide the velocity amplitude is approximately 1 m/s, and if we obtain the spring tidal amplitude from tidal tables (near the estuary mouth), then we obtain a depth estimate. However, this will be an overestimation of the depth, because the spring tidal amplitude is generally damped in an ideal estuary (whereas the neap tide amplitude is amplified) to asymptotically reach the ideal tidal amplitude. So assuming 1 m/s for the tidal velocity amplitude and the spring tidal amplitude from the tidal table would lead to an overestimation of the depth [see *Gisen et al.*, 2015]. But comparison with equation (6) will certainly help to make a better depth estimate.

With equation (11) we can estimate the channel roughness. If one assumes a velocity amplitude of 1 m/s at spring tidal range, equation (11) provides a first estimate of the roughness for an ideal estuary. Alternatively, equation (12) can be substituted into (11):

$$C^2 = r_s v \omega \frac{b_1^2}{h_1^2} \sqrt{\frac{c_0^2}{c_0^2 + \omega^2 b_1^2}} \quad (13)$$

after which the roughness entirely depends on the geometry, with the exception of the velocity amplitude, which may be assumed to be close to unity. This equation hinges strongly on the prediction of the estuary depth, which has a relatively large uncertainty. Therefore, this equation may be less accurate.

So in an ungauged estuary, knowing the width convergence and having an estimate of the depth by equation (6), the assumption of the ideal estuary allows us to obtain a first estimate of the tidal hydraulics, and particularly the tidal wave celerity (which is the same as c_0), the damping (which is zero), and the tidal velocity amplitude (which under ideal conditions should be somewhat less than 1 m/s). We can also determine the channel roughness from equation (11), and the phase lag between high water (HW) and high water slack (HWS) from equation (10), which in an ideal estuary purely depends on the convergence.

4. Predicting Salt Intrusion on the Basis of Estuary Shape

An often asked question to water managers is how much salt water intrusion one may expect in an estuary, especially as a result of planned upstream withdrawals. A full hydrometric survey to calibrate salt intrusion models is generally very costly and time demanding. A first estimate based on the procedure described here would not only provide an order of magnitude of the problem at hand, it could also provide the basis for a more intensive survey, whereby it is possible to home-in on the most important part of the estuary to be studied in more detail.

The procedure for determining the salt intrusion in ungauged estuaries is based on the work done earlier by *Savenije* [1986, 1993], which is summarized in *Savenije* [2005, 2012]. This procedure is based on the exponential shape of alluvial estuaries and on the method of *Van der Burgh* [1972], and uses two predictive equations for the two model parameters: the dispersion at the upstream boundary and the Van der Burgh shape coefficient. Recently, *Gisen et al.* [2015] reanalyzed the available database, including seven previously not surveyed Malaysian estuaries, and came up with revised predictive equations for the model parameters. These are the equations we present her.

The basis of the salt intrusion model is the steady state salt balance equation:

$$\frac{|Q_f|}{A}(S - S_f) + D \frac{dS}{dx} = 0 \quad (14)$$

where S is the tidal average salinity, Q_f is the freshwater discharge at the upstream boundary with salinity S_f , and D the dispersion coefficient. The latter is an essential model parameter that different authors have handled in very different ways. Most common is to link the parameter to the salinity gradient [e.g., *Prandle*, 1981] under the assumption that the dispersion is governed by gravitational, or density-driven, circulation [e.g., *Thatcher and Harleman*, 1972]. This process is indeed dominant in prismatic channels and flumes, on the basis of which much theoretical work has been done, but in natural channels, mixing is caused by a combination of tide-driven and density-driven circulation [e.g., *MacCready*, 2004]. Many researchers have tried to decompose all different dispersion processes in detail, sometimes distinguishing more than 60 components [Park and James, 1990].

Fortunately, in alluvial systems, the process is not that complex. Also, here a broader view, looking at the system as a whole, would help. Mixing is a process of relaxing gradients, to which also principles of maximum efficiency can be applied. The theoretical basis for this approach still needs to be provided, but fact is that alluvial estuaries appear to manifest predictive and relatively simple mixing behavior. The empirical equation of *Van der Burgh* [1972] is surprisingly simple, dimensionally correct, and appears to perform very well in practice. The coefficient K is a sort of shape factor determining the form of the salt intrusion curve:

$$\frac{dD}{dx} = -K \frac{|Q_f|}{A} \quad (15)$$

where K is Van der Burgh's coefficient, which can assume values between 0 and 1. Interestingly, it can be shown that D relates to the salinity gradient to the power $K/(1 - K)$. Combination of (14) and (15) results in $D \propto S^K$. Subsequent substitution into (14) results into D being proportional to dS/dx to the power $K/(1 - K)$:

$$\frac{D}{D_i} = \left(\frac{AD_i}{|Q_f|S_i} \frac{dS}{dx} \right)^{\frac{K}{1-K}} \quad (16)$$

where the subscript i refers to a boundary condition. If $K = 0.5$, then this power is 1; if $K = 2/3$, then the power is 2; if $K = 3/4$, then the power is 3, which are powers one finds in the literature [e.g., *MacCready*, 2004; *Prandle*, 1981], depending on the dominant mixing mechanism. The Van der Burgh coefficient, thus, allows the tuning of an estuary to the right combination of mixing mechanisms.

Combination of equations (14) and (15) yields an explicit expression for the salt intrusion (for the derivation see equations (5.43)–(5.48) in *Savenije* [2012]):

$$\frac{S - S_f}{S_i - S_f} = \left(1 - \frac{Ka_i|Q_f|}{D_iA_i} \left(\exp\left(\frac{x - x_i}{a_i}\right) - 1 \right) \right)^{1/K} \quad (17)$$

where $i = 0, 1$ represent the two segments of the estuary shape and D_i are the values of the dispersion coefficient at the mouth and the inflection point. In this approach the boundary condition is chosen at the inflection point (at $x = x_1$). The total salt intrusion length follows from equating the right hand member of equation (17) to 0 at $x = L$:

$$L = x_1 + a_1 \ln \left(\frac{D_i A_i}{K a_i |Q_f|} + 1 \right) \quad (18)$$

where L is the total salt intrusion length at tidal average condition. For the maximum intrusion at high water slack half a tidal excursion $E = vT/\pi$ needs to be added.

For given geometry and river discharge, these equations can be solved explicitly if values for K and D_1 are provided. If salinity observations along the estuary are available, then K and D_1 can be determined by calibration, but to use equation (17) in a predictive mode (providing the salinity distribution for a given river discharge and tide) predictive equations are needed. The reanalysis of *Gisen et al.* [2015] provided the following two equations ((19) and (20)) to be used in ungauged basins:

$$\frac{D_1}{v_1 E_1} = \alpha \left(\frac{\Delta \rho g h_1 |Q_f| T}{\rho v_1^2 A_1 E_1} \right)^{0.57} \quad (19)$$

where the argument is the estuarine Richardson number consisting of the densimetric Froude number and the Canter-Cremers number, and reflecting the balance between the potential energy of the river water over the kinetic energy of the tide. Here $\Delta \rho$ is the density difference between the salinity of sea and river water. The proportionality factor α depends on the channel roughness ($\alpha = 0.396(g/C^2)^{0.21}$). The channel roughness can be determined by equation (13), but otherwise a constant value of $\alpha = 0.117$ performs almost equally well.

The other predictive equation is for the Van der Burgh coefficient, which determines the shape of the curve, particularly the shape of the tail. *Gisen et al.* [2015], based on dimensionless numbers of 20 estuaries, revised the original equation of *Savenije* [1993] into:

$$K = 8.03 \times 10^{-6} \left(\frac{B_f^{0.30} g^{0.93} H_1^{0.13} T^{0.97} \pi^{0.71}}{B_1^{0.30} C^{0.18} v_1^{0.71} b_1^{0.11} h_1^{0.15} r_s^{0.84}} \right) \quad (20)$$

with a standard error of 0.11, and considering $0 < K < 1$. These are all parameters that depend directly on the topography, can be estimated ($r_s \approx 1.1$, $v \approx 1$ m/s), determined from tidal tables (T and H , being the tidal period and the spring tidal range $\approx 2\eta$) or determined with equations (6) and (11). A positive aspect of equation (20) is that the most uncertain parameters (C and h_1) have only small exponents, which prevents this equation from giving highly uncertain estimates. For details on the regression analysis and the reliability of the results, reference is made to *Gisen et al.* [2015].

5. A Fully Integrated Predictive Estuary Model, Dream or Reality?

The combined theory of shape, hydraulics, and salt balance provides a complete solution for prediction in ungauged estuaries, where all processes are determined by estuary shape, particularly the width, simply observable from a map. This is a rather remarkable finding, considering that estuarine processes are complex and intertwined. But maybe the answer lies in this complexity. The feedback mechanisms present in estuaries, where potential and kinetic energy from river flow and tide and chemical energy contained in the saline-freshwater gradient are dissipated, and where the estuary has the capacity to adjust its morphology, result in a predictable and simple shape, probably because the system operates close to its thermodynamic limit. Estuary shape is the result of the morphology finding a configuration where energy is dissipated in the most efficient way, and hence the shape holds the key to the simple behavior we observe. Similarly, the tendency of the system to approach an ideal estuary, where the tidal amplitude is constant, is the result of the most efficient way of dissipating energy and maintaining the most probable state in the estuary, where tidal energy is equally distributed. Also the balance between tide-driven and density-driven mixing, resulting in an efficient combination of mixing mechanisms along the estuary axis, well described by the Van der Burgh equation, is probably related with mixing efficiency. Of course this is mostly speculation, and still much has to be done to develop a closed theory

Table A1. Dimensionless Equations and Parameter Definitions

Phase lag equation	$\tan \varepsilon = \frac{\lambda}{\gamma - \delta}$ (A1)
Scaling equation	$\mu = \frac{\sin \varepsilon}{\lambda} = \frac{\cos \varepsilon}{\gamma - \delta}$ (A2)
Damping equation	$\delta = \frac{\mu^2}{\mu^2 + 1} (\gamma - \chi \mu^2 \lambda^2)$ (A3)
Celerity equation	$\lambda^2 = 1 - \delta(\gamma - \delta)$ (A4)
Shape number	$\gamma = \frac{c_0}{\omega b}$
Friction number	$\chi = r_s \frac{g}{C^2} \frac{c_0 \eta}{\omega h^2}$
Velocity number	$\mu = \frac{v}{c_s} \frac{\omega b}{\eta c_0}$
Damping number	$\delta = \frac{c_0}{\omega \eta} \frac{dv}{dx}$
Celerity number	$\lambda = \frac{c_0}{c}$

on integrated behavior. But there is enough empirical evidence to suggest that such a theory can be found.

Meanwhile, this paper provides a set of equations that are useful to provide first estimates on essential estuarine processes, which can be obtained by a simple desk study without the use of complex mathematical models. Not only can this be useful in situations where no funds are available for detailed field observations, it can also provide a basis for more detailed observations, where a field campaign would focus on areas of maximum uncertainty.

Appendix A : Dimensionless Equations and Parameter Definitions

Table A1 presents the four dimensionless hydraulic equations and the five dimensionless variables, where γ is the only independent variable. These variables consist of combinations of dimensional variables where c_0 is the classical celerity of a frictionless wave in a prismatic channel defined by $c_0 = \sqrt{gh_1/r_s}$, c is the actual phase speed (apparent wave celerity) in the estuary, r_s is the ratio of storage width to stream width (accounting for the fact that the tidal flats store water but do not contribute significantly to the longitudinal flow), C is the Chezy coefficient, η is the tidal amplitude, v is the tidal velocity amplitude, and $\omega = 2\pi/T$ is the tidal frequency, where T is the tidal period. The phase lag ε is the phase difference between high water (HW) and high water slack (HWS), or similarly between low water (LW) and low water slack (LWS).

Acknowledgment

The paper makes use of figures and data from the PhD thesis by Jacqueline Isabella Anak Gisen, defended at Delft University of Technology on 14 January 2015 (<http://repository.tudelft.nl/view/ir/uuid%3Aa4260691-15fb-4035-ba94-50a4535ef63d/>). I also would like to thank Erwin Zehe and one anonymous reviewer for their very detailed and constructive comments.

References

- Bruun, P., and F. Gerritsen (1960), *Stability of Coastal Inlets*, North Holland Publ., Amsterdam, Netherlands.
- Cai, H., and H. H. G. Savenije (2013), Asymptotic behavior of tidal damping in alluvial estuaries, *J. Geophys. Res. Oceans*, 118, 1–16, doi:10.1002/2013JC008772.
- Cao, S., and D. W. Knight (1996), Regime theory of alluvial channels based upon the concept of stream power and probability, *Proc. Inst. Civ. Eng. Water Mar. Energy*, 118, 160–167.
- Gisen, J. I. A. (2015), Prediction in ungauged estuaries, PhD thesis, Delft Univ. of Technol., Delft, Netherlands.
- Gisen, J. I. A., and H. H. G. Savenije (2015), Estimating bankfull discharge and depth in ungauged estuaries, *Water Resour. Res.*, doi:10.1002/2014WR016227, in press.
- Gisen, J. I. A., H. H. G. Savenije, and R. C. Nijzink (2015), Revised predictive equations for salt intrusion modelling in estuaries, *Hydrol. Earth Syst. Sci.*, 12, 739–770.
- Hrachowitz, M., et al. (2013), A decade of Predictions in Ungauged Basins (PUB): A review, *Hydrol. Sci. J.*, 58(6), 1–58, doi:10.1080/02626667.2013.803183.
- Kleidon, A., and M. Renner (2013), Thermodynamic limits of hydrologic cycling within the Earth system: Concepts, estimates and implications, *Hydrol. Earth Syst. Sci.*, 17, 2873–2892, doi:10.5194/hess-17-2873-2013.
- Kleidon, A., E. Zehe, U. Ehret, and U. Scherer (2013), Thermodynamics, maximum power, and the dynamics of preferential river flow structures at the continental scale, *Hydrol. Earth Syst. Sci.*, 17, 225–251, doi:10.5194/hess-17-225-2013.
- Kleidon, A., M. Renner, and P. Porada (2014), Estimates of the climatological land surface energy and water balance derived from maximum convective power, *Hydrol. Earth Syst. Sci.*, 18, 2201–2218, doi:10.5194/hess-18-2201-2014.
- Lacey, G. (1930), Stable channels in alluvium. Minutes, *J. Inst. Civ. Eng.*, 229, 259–292.
- MacCready, P. (2004), Toward a unified theory of tidally-averaged estuarine salinity structure, *Estuaries*, 27, 561–570.
- Park, J. K., and A. James (1990), Mass flux estimation and mass transport mechanism in estuaries, *Limnol. Oceanogr.*, 35(6), 1301–1313.
- Prandle, D. (1981), Salinity intrusion in estuaries, *J. Phys. Oceanogr.*, 11, 1311–1324.
- Savenije, H. H. G. (1986), A one-dimensional model for salinity intrusion in alluvial estuaries, *J. Hydrol.*, 85, 87–109.
- Savenije, H. H. G. (1993), Predictive model for salt intrusion in estuaries, *J. Hydrol.*, 148, 203–218.
- Savenije, H. H. G. (2005), *Salinity and Tides in Alluvial Estuaries*, Elsevier, N. Y.
- Savenije, H. H. G. (2012), *Salinity and Tides in Alluvial Estuaries*, 2nd completely revised ed. [Available at salinityandtides.com.]
- Savenije, H. H. G., and E. J. M. Veling (2005), The relation between tidal damping and wave celerity in estuaries, *J. Geophys. Res.*, 110, C04007, doi:10.1029/2004JC002278.
- Savenije, H. H. G., M. Toffolon, J. Haas, and E. J. M. Veling (2008), Analytical description of tidal dynamics in convergent estuaries, *J. Geophys. Res.*, 113, C10025, doi:10.1029/2007JC004408.
- Simons, D. B., and M. L. Albertson (1960), Uniform water conveyance channels in alluvial material, *J. Hydraul. Div. Am. Soc. Civ. Eng.*, 86(5), 33–71.
- Thatcher, M. L., and D. R. F. Harleman (1972), A mathematical model for the prediction of unsteady salinity intrusion in estuaries, *R. M. Parsons Lab. Rep. 144*, MIT, Cambridge, Rijkswaterstaat, Netherlands.
- Van der Burgh, P. (1972), Ontwikkeling van een methode voor het voorspellen van zoutverdelingen in estuaria, kanalen en zeeën [in Dutch], *Rijkswaterstaat Rapp.* 10–72.